Institución Universitaria
Reacreditada en Alta Calidad
80 Años

Boletín Informativo

Departamento de educación y Ciencias Básicas

2024 - 3

Notas científicas, informativas y más.

Nota Informativa

Profesor
Ramiro Humberto Hoyos Zuluaga

El seminario permanente CONCIENCIA ITM que hace presencia institucional a nivel divulgativo en ciencia y tecnología desde la Facultad de Ciencias Exactas y Aplicadas a través del Departamento de Educación y ciencias Básicas, ha desarrollado el primer seminario titulado: Modelado de la calidad del aire en el Valle de Aburrá usando una red de sensores de bajo costo y asimilación de datos. Estuvo a cargo del doctor en Ingeniería Matemática Santiago López Restrepo.
A continuación, exponemos un breve resumen de su charla.

El uso de redes de calidad del aire de bajo costo ha ido en aumento en los últimos años para estudiar las dinámicas de la contaminación urbana. Aquí mostraremos la evaluación de la red operativa de bajo costo del Valle de Aburrá en comparación con la red oficial de monitoreo.

los resultados muestran que las mediciones de PM2.5 de bajo costo son muy cercanas a las observadas por la red oficial. Además, la red de bajo costo permite una mayor representación espacial de las concentraciones en todo el valle. Integramos las observaciones de bajo costo con el modelo de transporte químico Long Term Ozone Simulation-European Operational Smog (LOTOS-EUROS) utilizando asimilación de datos.

Se asimilaron dos configuraciones diferentes de la red de bajo costo: usando toda la red de bajo costo (255 sensores) y una selección de alta calidad usando solo los sensores con un factor de correlación mayor a 0.8 respecto a la red oficial (115 sensores). Las estaciones oficiales también fueron asimiladas para comparar el impacto de la red de bajo costo más densa en el rendimiento del modelo. Nuestros resultados sugieren que, con los avances actuales en sensores de bajo costo, es posible mejorar el rendimiento del modelo con la asimilación de datos de la red de bajo costo.

La siguiente es la programación del Seminario Permanente de la Facultad de Ciencias Básicas para este semestre 2024-02, están cordialmente invitados.

FACULTAD DE CIENCIAS EXACTAS Y APLICADAS
Departamento de Educación y Ciencias Básicas
Seminario Permanente CONCIENCIA ITM

Programación 2024-02

1. **Título:** Modelado de la calidad del aire en el Valle de Aburrá usando una red de sensores de bajo costo y asimilación de datos
   Ponente: Santiago López Restrepo
   Fecha: jueves 29 de agosto
   Hora: 10:00a.m. -12:00m
   Lugar: Aula Magna

2. **Título:** Ptencial Antitumoral del cannabidiol-CBD en cáncer colorrectal: una aproximación utilizando modelos in vitro.
   Ponente: Diego Uribe Yunda
   Fecha: jueves 26 de septiembre
   Hora: 10:00 a.m. -12:00m
   Lugar: Aula Magna

3. **Título:** Fundamentos de las Redes Neuronales
   Ponente: Luis Eduardo Nospiran Herrera
   Fecha: jueves 24 de octubre
   Hora: 10:00 a.m. -12:00m
   Lugar: Aula Magna

4. **Título:** Una breve historia sobre ondas y luz
   Ponente: Javier Vargas Valencia
   Fecha: jueves 14 de noviembre
   Hora: 10:00 a.m. -12:00m
   Lugar: Aula Magna

Nota Científica

Profesora
Johana Trochez González

SPECTRAL CHARACTERIZATION OF AVOCADO *PERSEA AMERICANA MILL CV. HASS* USING SPECTROMETRY AND IMAGERY IN THE VISIBLE TO NEAR-INFRARED RANGE

Maria C. Torres-Madronero[1], Tatiana Rondon[2], Ricardo Franco[3], Maria Casamitjana[4], Johana Trochez Gonzalez[5]

Abstract

Remote sensing technologies, such as spectral imagery, have great potential for crop monitoring. Spectral systems measure the reflected and emitted energy of a surface, usually between the visible and near-infrared ranges of the electromagnetic spectrum. This study presents a spectral characterization of avocado *Persea Americana Mill cv. Hass* using spectrophotometry and spectral imaging. *In situ* data collected with spectrometers and greenseekers, and remote data from sensors onboard satellites such as Landsat 8 and Sentinel 2 were analyzed. This study is performed over four productive units of avocado. First, the shape of the spectral signatures captured for the *in situ* and remote sensors was compared and subsequently related to their vegetation indices. Differences between young and mature leaves were established using spectrometry, mainly between 480 and 650 nm. This spectrum region showed the color changes of young avocado leaves. From satellite data, the spectral signature presents significative differences between Sentinel 2 and Landsat 8. The results suggest that these differences can be due to several factors, such as the date of acquisition, pre-processing, and spatial resolution. Finally, vegetation indexes from *in situ* and satellite measurements show different scales. The normalized difference vegetation index (NDVI) for *in situ* data ranged between 0.9 and 0.7 for the spectrometer and greenseeker, respectively. However, the derived NDVI from satellite data is around 0.4 for Sentinel 2 and 0.3 for Landsat 8.

Keywords

Avocado, multispectral imagery, remote sensing, spectrometry, vegetation indexes.

1. INTRODUCTION

Remote sensing uses sensors, systems, and models to characterize the Earth's surface. The growing interest in this field drives the development of several optical sensors and platforms with different spatial, spectral, and temporal resolutions [1]-[3]. Among the multispectral systems are Landsat 8 of NASA and Sentinel 2 of the European Special Agency (ESA); both platforms include multispectral cameras that collect between 8 to 13 bands from the visible to the short infrared spectral range [4]. The spectral response of a surface can be used to characterize the materials and objects in the sensor field of view. Among the application of multispectral remotely sensed imagery are cartography [5], weather studies [6], defense and security [7], mining [8], agriculture [9], and others. Remarkably, precision agriculture has a growing interest in these systems since they provide information in several electromagnetic spectrum bands, and multispectral systems can sense large fields of crops. However, although the spectral response of the vegetation signature is one of the most studied, it is also one of the most complex [10].

A low reflectance characterizes the visible region of a spectral signature from vegetation due to leaf pigments and chlorophyll absorption [10]. The vegetation spectrum presents the red edge, the most discriminant feature between 690 nm and 720 nm [10]. In this region, there is a significant increment of reflectance. This behavior is associated with the internal structure of leaves and water content. Finally, vegetation has higher reflectance in the near-infrared [10]. The shape of the spectral signature is affected by the physiological and health conditions of the plants. Several methods studied the relation between the vegetation spectral response and environmental, geographic, and phenological conditions [11]-[13]. These methods can be grouped into three approaches: vegetation indexes, parametric models, and non-parametric models.

Vegetation indexes (VI) are band ratios derived from the discriminant features of the vegetation spectrum [12]. Usually, VI is based on two or four bands; thus, these have a low computational cost. VI is commonly used to estimate leaf area, chlorophyll content, biomass, yield, and others. The most used VI is the normalized difference vegetation index (NDVI), a function of the reflectance in the near-infrared and red spectral bands. This index is between -1 and 1 [12],[14]. Some studies have shown that the NDVI for a healthy plant is higher than 0.66. There are several proposed VI in the literature. The simplicity of calculation from spectrometry and imagery has led to their massive use.

However, it is necessary to be careful with the interpretation of VI because they only use a limited number of spectral bands.

An alternative to vegetation indexes is biophysical models, which explore the interaction of light with plants in terms of their biophysical characteristics [15]. Biophysical models describe spectral variation as a function of cover, leaf, and soil characteristics [15]. Estimating biophysical characteristics depends on an inversion process, which minimizes the difference between actual and simulated data. Previous work has shown that the inversion of such transfer models from remotely sensed data is computationally expensive, highly complex, and limited by the resolution of cameras [15]. Biophysical models include the SAIL model for bidirectional reflectance of plant cover and PROSPECT, which models the optical properties of leaves.

Unlike parametric models, non-parametric models do not require the assumption of band relations or knowledge of the data distribution. In this sense, new techniques for extracting biophysical features from methods such as neural networks, random forests, and support vector machines are found in the literature. For example, Verrelst et al. [16] used techniques based on Gaussian processes to study each band of a spectrum, as well as the entire spectrum, to estimate biophysical parameters such as chlorophyll, leaf area index, and plant cover fraction [16]. Estimating biophysical parameters from a set of relevant bands reduces the computational cost of parametric methods. Additionally, it allows an understanding of the relationship of spectral signatures with the optical properties of plants.

There are few studies about the avocado spectral response. In [17], it was demonstrated that it is possible to classify diseased trees with phytophthora and healthy trees using bands between 400 and 950 nm from data captured in the laboratory. However, there are no field studies that validate these results. In [18], hyperspectral images are used to characterize avocado ripening. Sankaran et al. [19] used spectral signatures from 350 nm to 1000 nm and VI to classify healthy, asymptomatic, and symptomatic leaves infected by laurel wilt.

Despite the advance in the study of the vegetation spectral response, understanding physiological, phenological, and health effects in the signatures require specific studies since they depend on environmental conditions and the specie itself. Thus, this paper seeks to obtain a spectral characterization of avocado *Persea Americana Mill cv. Hass*, using both spectrometry and multispectral imagery. The spectral characterization includes the comparison of some standard VI and the effects of scale by using directly collected spectral signatures and satellite data.

2. MATERIALS AND METHODS

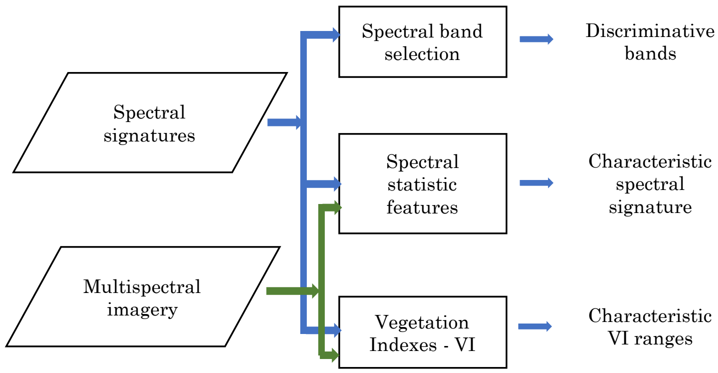

Figure. 1. Framework to establish the spectral characterization of avocado *Persea Americana Mill cv. Hass* using spectral signatures and multispectral images in the visible and near-infrared range.

The spectral characterization of avocado *Persea Americana Mill cv. Hass* is presented in two scales. The first scale used spectral signatures collected directly in the leaf trees in the visible to near-infrared range. This scale has a high spectral resolution but requires considering the differences between young and mature leaves. Signatures collected in productive units are used to understand the spectral response of avocado, identifying relevant spectral bands and the behavior of VI. On the other hand, the second scale analysis is performed using multispectral satellite data with different spatial resolutions. This second scale has a lower spectral and spatial resolution. Still, it intends to understand the spectral feature of avocado in a more generalized way that can be used in future studies for the estimation, detection, and monitoring of these crops. Figure 1 presents the methodology implemented in this paper, described in detail in the following sections.

2.1 Spectral data

This study was focused on the spectral response of *Persea Americana Mill cv. Hass*. This is a vigorous tree with lateral branching. The axillary buds develop into branches through the elongation and enlargement of internodes and expansion of the leaves. *Persea Americana Mill cv. Hass* leaves have different mature stages associated with their color, size, and shape (Figure 2). The apical leaves of the branches are considered young leaves. These young leaves emerge from a breaking bud, stem node, or growing stem tip so that the petiole is visible at its point of attachment to the stem. Instead, mature leaves have reached the full size or turned a darker green color or tougher texture [20]. For this reason, we collected both young and adult leaves to study their spectral signature.

Leaves were collected from avocado trees on four farms in eastern Antioquia between the municipalities of Rionegro and El Retiro. Table 1 summarizes the geolocation of the farms used for this study. On each farm, 60 young leaves and 60 mature leaves were collected. Figure 2 presents the variability between young and mature leaves obtained in the data set. On the left of the image are the youngest leaves, and the oldest ones are on the right. Spectral signatures were captured using an Ocean Insight FLAME S VIS NIR ES spectrometer and a QP600-2-VIS-BX fiber. This device captures 2048 spectral bands between 339 to 1028 nm with a resolution of 1.33 nm. 10 spectral signatures are captured and averaged for each leave to reduce noise.

Table 1. Geolocation of farm. Source: Created by the authors.

No.	Polygon Coordinates	Area	Young leaves Original/Cleaned	Mature leaves Original/Cleaned
1	N 6.09618 W-75.46996 N 6.09599 W-75.46973 N 6.09585 W-75.46998 N 6.09606 W-75.47036	1996 m^2	60/60	60/60
2	N 6.1127 W-75.403761 N 6.11177 W-75.40241 N 6.11028 W-75.40343 N 6.11081 W-75.40516	48351 m^2	60/59	60/58
3	N 6.10909 W -75.393110 N 6.109530 W-75.388717 N 6.106598 W-75.386603 N 6.106737 W-75.393000	219323 m^2	60/56	60/58
4	N 6.03423 W-75.37977 N 6.02930 W-75.37309 N 6.02601 W-75.37972 N 6.02923 W-75.38625 N 6.03316 W-75.38629	938536 m^2	60/60	60/60

Total	240/235	240/236

Figure. 2. Variability among young leaves (left side) and mature leaves (right side). Source: Created by the authors.

For calibration, the spectral response of both a white and a black pattern is captured before and after the acquisition, r_{white} and r_{black}, respectively. Finally, the reflectance for each leaf, $R(\lambda)$, is obtained using equation (1), where λ represents the wavelength and r the measured radiance.

$$R(\lambda) = \frac{r(\lambda) - r_{black}(\lambda)}{r_{white}(\lambda) - r_{black}(\lambda)} \tag{1}$$

The used spectral bands ranged between 480 nm and 900 nm for the spectral characterization of avocado *Persea Americana Mill cv. Hass* since other spectral bands present a low signal-to-noise ratio. The spectral signatures in this range are filtered with a uniform sliding window filter using 10 points. The uniform filter helps to reduce the noise and preserve the shape of the signatures. Finally, the mean and standard deviations were calculated to remove corrupted signals from the collection. The final number of samples per farm is presented in Table 1.

2.2 Multispectral imagery

The spectral responses of avocado leaves collected *in situ* were compared with the spectral signatures captured by the multispectral satellite sensors Sentinel 2 and Landsat 8. Sentinel 2 is a mission of the European Space Agency (ESA) that includes two polar-orbiting satellites with multispectral cameras. The multispectral imagery consists of 13 bands from 443 nm to 2190 nm. The spatial resolution depends on the spectral band: images of 10-meter spatial resolution are collected in B2 (490 nm), B3 (560 nm), B4(665 nm), and B8 (842 nm), and 30-meter imagery is collected in B5 (705 nm), B6 (740 nm), B7 (783 nm), B8a (865 nm), B11 (1610 nm), and B12 (2190 nm), and 60 meters imagery for B1 (443 nm), B9 (940 nm), and B10 (1375 nm). The level 2A products of Sentinel 2 are freely available and consist of bottom reflectance with geometric and radiometric corrections. This study used the image captured on May 8, 2022. An RGB image composition using B4, B3, and B2 over the study zone is presented in Figure 3a.

On the other hand, Landsat 8 satellite from NASA includes a multispectral system that measures from the visible to the shortwave infrared spectral range. Landsat 8 imagery includes one panchromatic image with 15 meters (500 nm - 650 nm) and eight bands with a spatial resolution of 30 meters: B1 coastal aerosol (430 nm - 450 nm), B2 blue (450 nm - 510 nm), B3 green (530 nm - 590 nm), B4 red (650 nm - 670 nm), B5 near-infrared (850 nm - 889 nm), B6 SWIR 1 (1570 nm - 1650 nm), B7 SWIR 2 (2110 nm - 2290 nm), and B9 cirrus (1350 - 1380 nm). The data includes the surface reflectance image obtained after the atmospheric correction. This study used the Landsat 8 image captured on Jan 8, 2022. An RGB composition using the B4, B3, and B2 is presented in Figure 3b. No low cloud cover images were found closer to the collection date of spectral signatures.

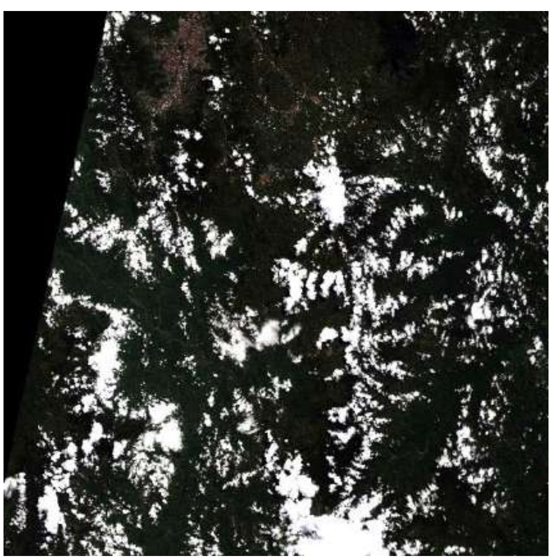

(a)

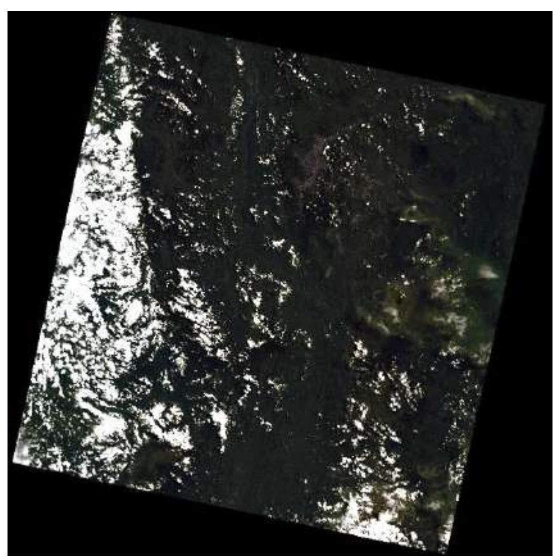

(b)


(c)


(d)

Figure. 3. RGB composition for (a) Sentinel 2 image captured on May 8, 2022, using B4(665 nm), B3 (560 nm), and B2 (490 nm), (b) Landsat 8 image captured on Jan 8, 2022, using B4 red (650 nm - 670 nm), B3 green (530 nm - 590 nm), and B2 blue (450 nm - 510 nm). Image subset including the four farms from (c) Sentinel 2 and (d) Landsat 8. Images downloaded from Earth Explorer (https://earthexplorer.usgs.gov/). Source: Created by the authors.

2.3 Processing and analysis of spectral signatures

This study aims to establish a spectral characterization of avocado *Persea Americana Mill cv. Hass* in the visible to near-infrared range. Three different analyses of the spectral signatures were realized from data collected in eastern Antioquia (Colombia) farms. The first analysis consisted of a statistical approach: separating the spectra by farm and using the whole dataset. In this statistical analysis, first and second-order statistics are computed. The *in situ* spectral signatures are compared with the overall spectral response measured by Landsat 8 and Sentinel 2 systems.

Then, discriminative spectral bands were determined using subset-band selection algorithms (SSBS). An algorithm based on singular value decomposition (SVD) proposed by Velez and Jimenez [21] was implemented. This algorithm is unsupervised and requires the number of bands p. Given the set of spectral signatures S as the input parameter, the algorithm computes the SVD of the covariance matrix of S and selects the first p eigenvectors. Then, a QR factorization is applied, pivoting over the set of selected eigenvectors. The p first elements of the pivoting are used as the most relevant bands.

Finally, the behavior of spectral signatures of avocado *Persea Americana Mill cv. Hass* leaves was determined using several VI. Table 2 summarizes the VI used in this paper. These VI use wavelengths in our signature range and, according to the literature, are related to plant health. The VI uses the bands: red (R), green (G), blue (B), red edge (RE), and near-infrared (NIR). Since the collected spectral signatures have a high resolution, the mean reflectance in the wavelength ranges of Landsat 8 was obtained. Thus, B is the mean

reflectance between 450 nm and 510 nm, G between 530 nm and 590 nm, R between 630 nm and 670 nm, and NIR between 850 nm and 880 nm. The range between 730 nm and 740 nm was used to obtain the reflectance of RE. A comparison between the vegetation indices obtained using the *in situ* measurement and the satellite data was made only with the VI that can be computed from the Landsat 8 and Sentinel 2 images.

Table 2. Selected vegetation indices used to study spectral signatures from avocado *Persea Americana Mill cv. Hass*. Source: Created by the authors.

VI	Equation	Reference	Description
NDVI - Normalized Difference Vegetation Index	$\frac{NIR - R}{NIR + R}$	[14]	Vegetation health and growth
NDRE – Normalized difference red edge	$\frac{NIR - RE}{NIR + RE}$	[22]	Chlorophyll content
OSAVI - Optimized soil adjusted vegetation index	$\frac{NIR - R}{NIR + R + 0.16}$	[23]	Minimized effects of soil variation
MCARI – Modified Chlorophyll Absorption Ratio Index	$\frac{(RE - R) - 0.2(RE - G)}{RE/R}$	[24]	Chlorophyll content
MTCI – Meris terrestrial chlorophyll index	$\frac{NIR - RE}{RE - R}$	[25]	Sensitive to nitrogen

R: red band. G: green band. NIR: near-infrared band; RE: red edge band.

3. RESULTS AND DISCUSSION

3.1 Spectral characterization of avocado *Persea Americana Mill cv. Hass*

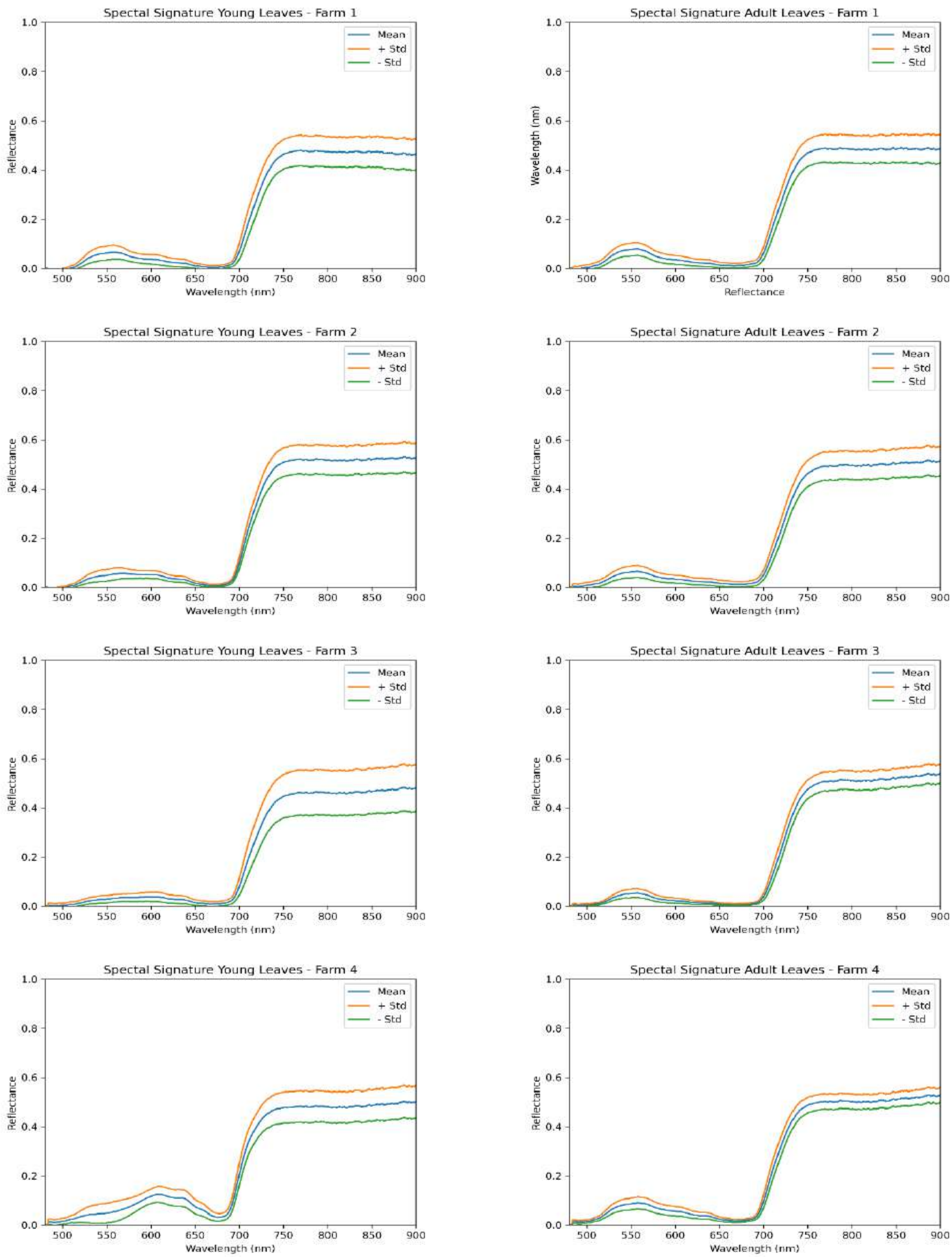

Figure. 4. Spectral signatures from avocado *Persea Americana Mill cv. Hass* for each farm. Left column: young leaves. Right column: mature leaves. +Std corresponds with the mean spectrum plus one standard

deviation, and -Std corresponds with the mean spectrum less one standard deviation. Source: Created by the authors.

First, the spectral behavior of avocados was analyzed on each farm and establish the differences between the young and mature leaves. Figure 4 presents the mean spectral signatures and their standard deviation for young (left column) and mature (right column) leaves. In the first farm, it can be noted that the reflectance peak, due to the leaf pigments, is at 550 nm for both young and mature leaves; the red edge begins before 700 nm and ends at 750 nm. For farms 2, 3, and 4, Figure 4 shows the differences between young and adult leaves. For instance, chlorophyll absorption increases from 600 nm for young leaves and 550 nm for mature leaves.

On the other hand, it can be seen in Figure 4 a higher standard deviation for young leaves than for mature leaves. Generally, at 550 nm, the spectral signature shows more significant variation in qualitative terms between young and mature leaves. This is because the mature leaves show a dull deep green color, while the young leaves show a wide range of colors, some bright, ranging from brown, reddish, light green, yellow, and a combination of these in the same leaf.

An analysis of the entire dataset without considering the farms was realized. Figure 5 compares the mean spectral signature obtained from young and mature leaves. Considering all wavelengths, the similarity calculated with the cosine distance between the young and mature signatures was 0.9974. Figure 6 explores with more detail the differences in three spectral regions: (I) 480 nm to 650 nm (Figure 6a), (II) 650 nm to 750 nm (Figure 6b), and (III) 750 nm to 900 nm (Figure 6c). The main differences between young and mature leaves in the visible region are between 480 nm to 650 nm (similarity of 0.9160). This region is related to leaf pigments and chlorophyll absorption. In the visible region, the higher reflectance for young leaves is near 550 nm, but for mature, leaves are near 600 nm. In the red edge region (650 nm to 750 nm), a shift at the beginning of the red edge between the young and mature leaves (similarity of 0.9934) was noticed. Finally, the difference is only amplitude in the near-infrared region (650 nm to 750 nm, similarity of 0.9999). The avocado plant is characterized by presenting different phenological states in its crown. For instance, in commercial plantations, a plant simultaneously presents a development and fruiting phase. This generates different colors at the same time in the foliage.

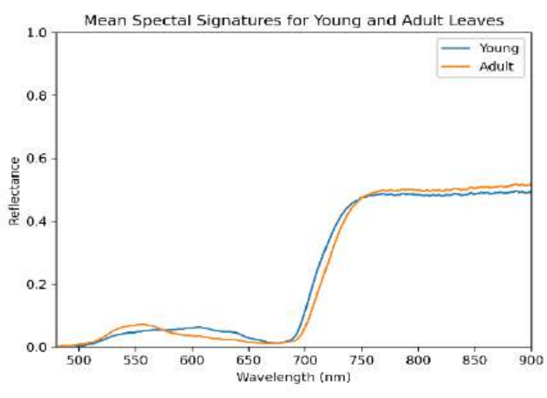

Figure. 5. Comparison of spectral signatures between young and mature leaves of avocado *Persea Americana Mill cv. Hass*. Source: Created by the authors.

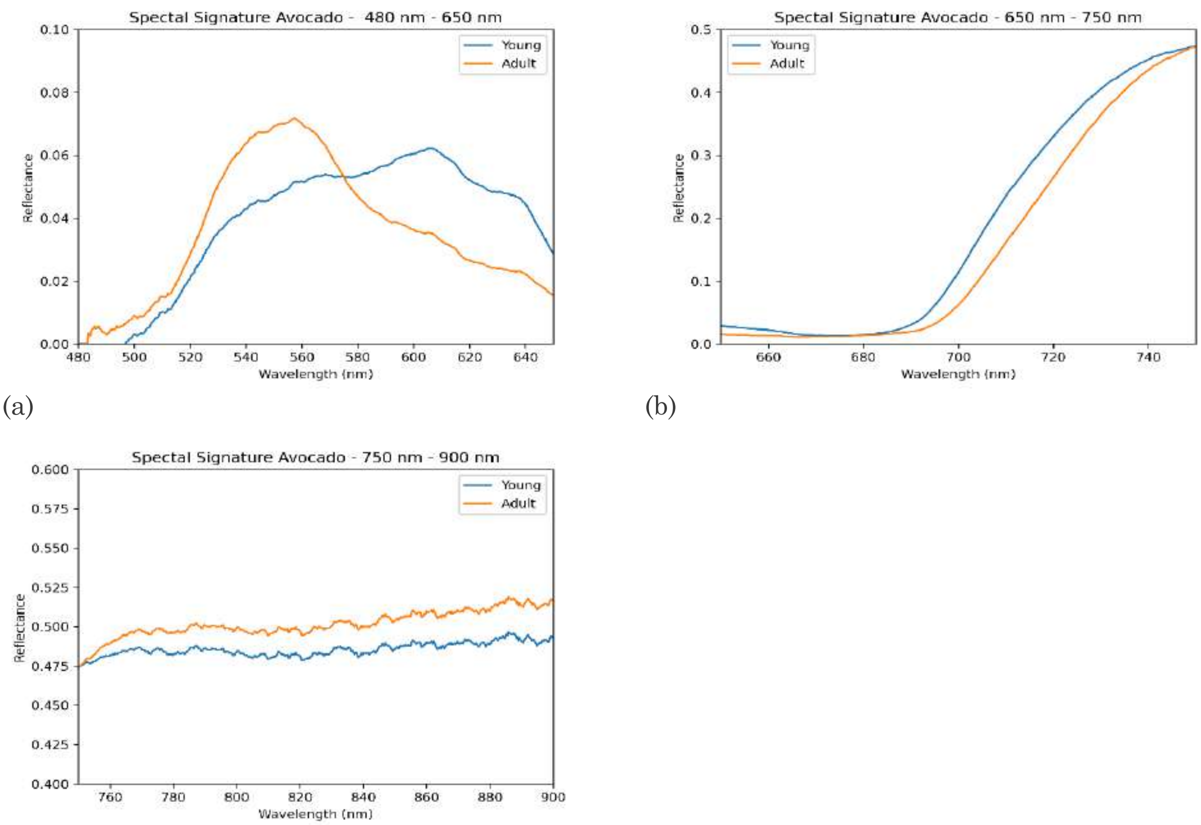

(a) (b)

(c)

Figure. 6. Detailed comparison of spectral signatures between young and mature leaves of avocado *Persea Americana Mill cv. Hass* in the different spectral ranges: (a) 480 nm to 650 nm, (b) 650 nm to 750 nm, (c) 750 nm to 900 nm. Source: Created by the authors.

3.2 Comparison of spectral signatures from *in situ* measurement and satellite data

The spectral signatures were obtained from the satellite imagery collected by Sentinel 2 and Landsat 8. Figure 7(a) presents the spectral signatures from Sentinel 2 for the four farms in the bands B2, B3, B4, and B8, which have 10 meters of spatial resolution. On the other hand, Figure 7(b) presents the signatures using the five bands of Landsat 8 (B1, B2, B3, B4, B5) that have 20 meters of spatial resolution. In this scale of analysis, differences between young and mature leaves cannot be observed. In addition, Figure 7(c) compares the mean spectra from Sentinel 2 and Landsat 8, combining the four farms. The signatures show variability between the two sensors. These variations can result from several factors, such as date of acquisition, atmospheric and radiometric corrections, and spatial resolution.

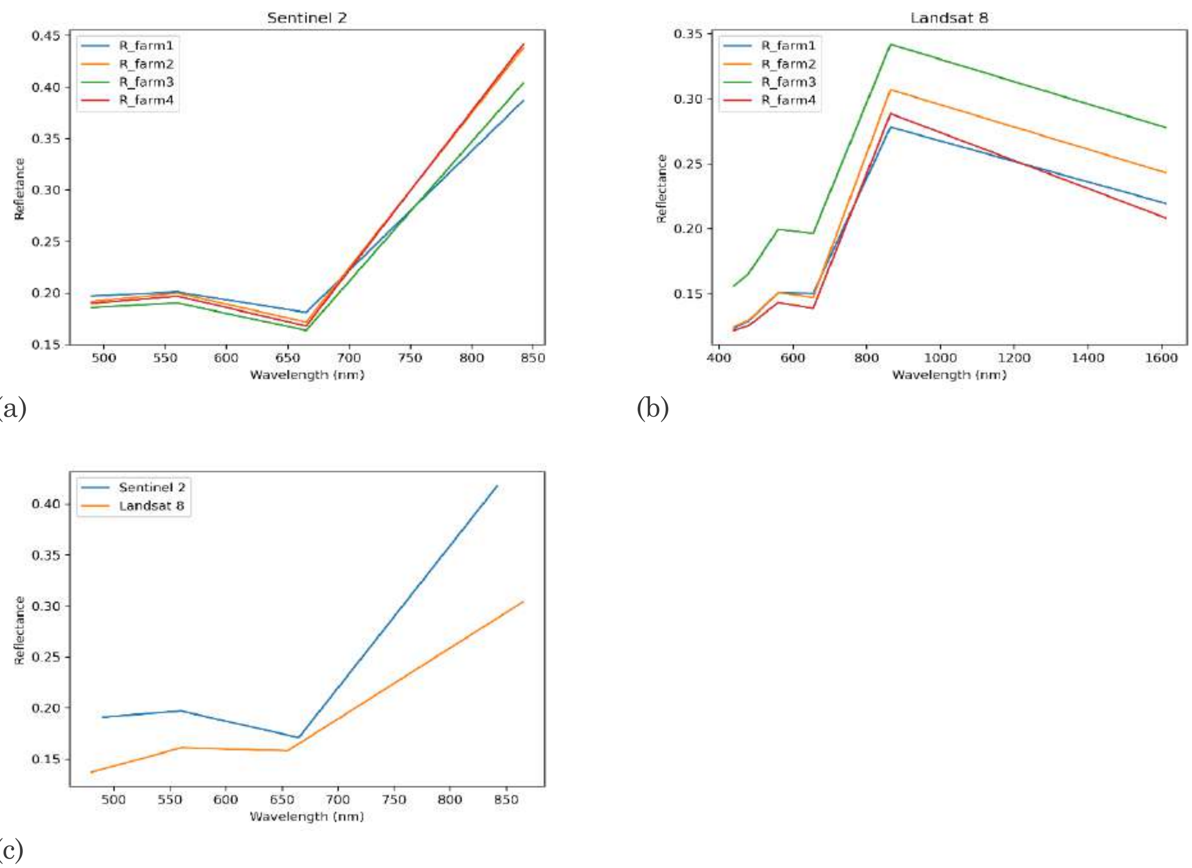

Figure. 7. Comparison of spectral signatures of farms collected by (a) Sentinel 2 and (b) Landsat 8. (c) Mean spectra for all farms obtained from Sentinel 2 and Landsat 8. R_farm$i$ refers to the mean reflectance obtained from farm i. Source: Created by the authors.

3.3 Spectral band selection

Comparing the results obtained from satellite data and close-range spectrometry, it can be noted the differences between these two kinds of scale. The satellite sensors include relevant bands for vegetation characterization, such as the NIR and red bands. However, their lower spatial and spectral resolution limits the analysis of plants. Then, we used SBSS algorithms to determine relevant bands for avocado signatures. Results obtained in section 3.1 suggest that the visible range is relevant for this plant. The unsupervised SBSS algorithm based on SVD was used to validate these results. Table 3 presents the ten most relevant bands selected by the SVD-based algorithm. Figure 8 shows the spectral signatures of young and mature leaves of avocado with the selected bands overlayed. Note that ten bands are between 480 nm and 650 nm. Figure 8 identifies five relevant regions: close 500 nm, 540 nm, 540 nm, 610 nm, and 630 nm.

Table 3. Selected first ten relevant bands using SVD based algorithm and the spectral signatures from avocado *Persea Americana Mill cv. Hass*. Source: Created by the authors.

	Number of band	Wavelength		Number of band	Wavelength
1	218	559.3983	6	348	605.5922
2	434	635.7183	7	0	480.2063
3	199	552.5817	8	159	538.1772
4	209	556.1714	9	164	539.9818
5	37	493.7973	10	46	497.0939

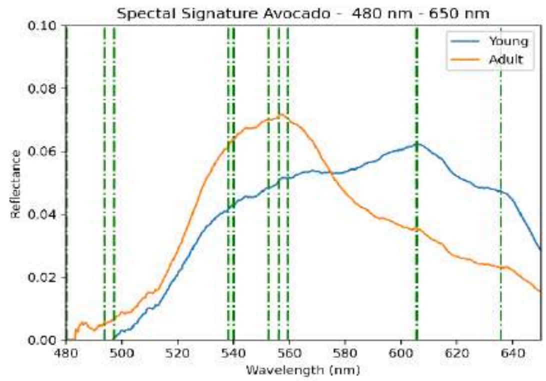

Figure. 8. Spectral signatures of young and mature leaves of avocado *Persea Americana Mill cv. Hass* between 480 nm and 650 nm with selected relevant band by SVD-based algorithm. Source: Created by the authors.

3.4 Vegetation Indexes

Figure 9 compares the VI obtained from the young and mature leaves of avocado using the *in situ* measurements. Table 4 presents the mean, median, and standard deviation (σ) for the computed VI. Figure 9 shows that young leaves have a higher dispersion of NDVI, OSAVI, and MCARI values than mature ones. For instance, the NDVI mean value for young leaves was 0.8866 with σ=0.2057, and for mature, leaves were 0.9369 with σ=0.0398. On the other hand, the NDRE and MTCI reached higher dispersions on mature leaves than the younger ones. For instance, the NDRE mean value for young leaves was 0.0645 with σ=0.0358, and for mature leaves was 0.1186 with σ=0.0426. The outliers shown in Figure 9 represent the wide range of color in young leaves, with some exceptions in mature leaves, mainly due to the brightness of the dark green color.

Table 4. Mean, median, and standard deviation of vegetation indices – VI for young and mature leaves of avocado *Persea Americana Mill cv. Hass*. Source: Created by the authors.

VI	Mean		Median		Std. Deviation	
	Young	Mature	Young	Mature	Young	Mature
NDVI	0.8866	0.9369	0.9287	0.9426	0.1057	0.0398
NDRE	0.0645	0.1186	0.0588	0.1078	0.0358	0.0426
OSAVI	0.6728	0.7164	0.7059	0.7196	0.0756	0.0292
MCARI	0.0217	0.0132	0.0148	0.0120	0.0189	0.0086
MTCI	0.1486	0.2856	0.1297	0.2563	0.0875	0.1154

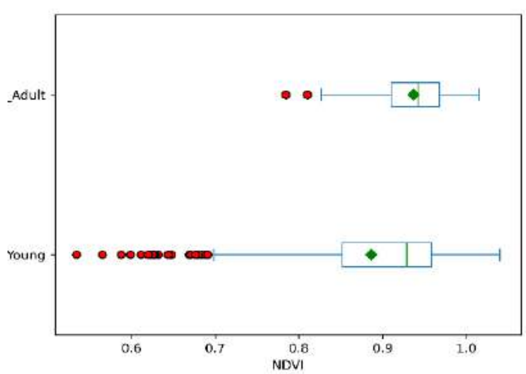

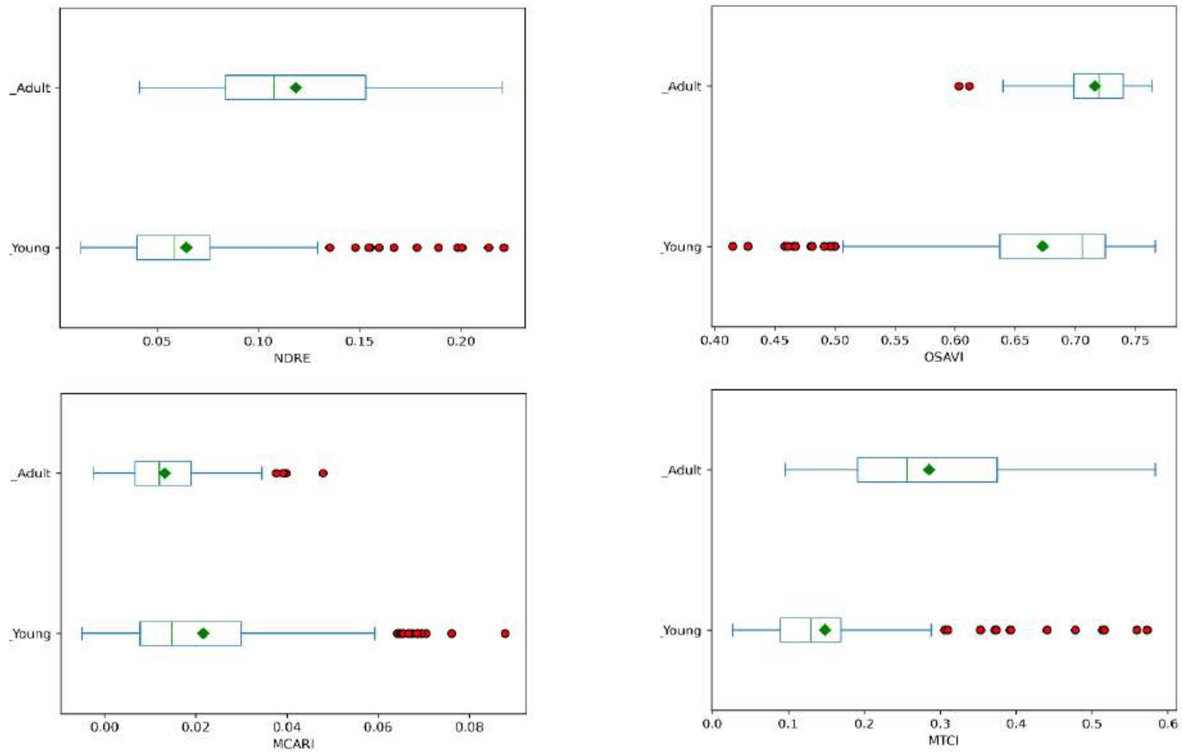

Figure. 9. Vegetation indexes for young and mature leaves of avocado *Persea Americana Mill cv. Hass*. Source: Created by the authors.

3.5 Comparison of vegetation indexes derives from satellite data

Table 5 presents the NDVI and OSAVI obtained from spectral signatures derived from multispectral satellite imagery. In this case, the obtained NDVI for the avocado farms using Sentinel 2 was around 0.4 instead the 0.9 value obtained for close-range signatures. For Landsat 8, the NDVI value was around 0.3. Compared with the close-range spectra, these lower values can also be due to the spectral and spatial resolutions and atmospheric effects.

Table 5. Mean and standard deviation of vegetation indices – VI from farms on study area derived from Sentinel 2 and Landsat 8 images. Source: Created by the authors.

VI		Sentinel 2		Landsat 8	
		Mean	Std. Deviation	Mean	Std. Deviation
NDVI	Farm 1	0.3642	0.0583	0.2981	0.0644
	Farm 2	0.4303	0.0859	0.3465	0.0876
	Farm 3	0.4193	0.0576	0.2830	0.0842
	Farm 4	0.4449	0.0772	0.3480	0.0759
OSAVI	Farm 1	0.2835	0.0442	0.2170	0.0476
	Farm 2	0.3414	0.0727	0.2570	0.0682
	Farm 3	0.3271	0.0500	0.2149	0.0586
	Farm 4	0.3527	0.0649	0.2535	0.0579

3.6 Comparison of vegetation indexes measured with GreenSeeker

Table 6 presents the mean and standard deviation for the measurements of NDVI collected using the GreenSeeker. Using this equipment, the mean of mature leaves was around 0.7225, but for young leaves was around 0.4550. These measurements are lower than the estimated from spectral signatures collected by the field spectrophotometer. However, differences in NDVI are evident between young and mature leaves, thus demonstrating the tool's sensitivity. Gutierrez-Soto et al. [26] indicate that the GreenSeeker equipment allows the determination of differences in a simple numerical index (NDVI) which reflects the physiological state of the crops in the field.

Table 6. Mean and standard deviation of NDVI for young and mature leaves of Hass avocado obtained using the GreenSeeker equipment. Source: Created by the authors.

VI	Mean		Std. Deviation	
NDVI	Young	Mature	Young	Mature
Farm 1	0.4500	0.7600	0.0724	0.0425
Farm 2	0.5000	0.7200	0.0675	0.0435
Farm 3	0.4300	0.7550	0.0350	0.0412

Farm 4	0.4400	0.6750	0.0337	0.0408
Mean	**0.4550**	**0.7225**	**0.0591**	**0.0463**

3.7 Discussion

One of the findings of this study is the characterization of the avocado *(Persea Americana Mill cv. Hass)* plant signature. The avocado spectral signature varies depending on the mature leaf stages (young and mature). In the case of young leaves, there is a more significant variety of colors in the visible region. Bands around 490, 540, 560, 605, and 635 nm are relevant for the spectral characterization of avocado, according to the results obtained.

Spectral characterization from multispectral satellite imagery shows little consistency between data captured by Sentinel 2 and Landsat 8. Both selected images include geometric, radiometric, and atmospheric correlation. However, the difference in capture date, pre-processing algorithms, and the spatial and spectral resolution of the data may affect the signatures. Premilitary works present spectral characterization of avocado trees using sentinel 2 [28] and fruit [18]. However, any studies that publish spectral signatures captured directly on the plant can be found.

On the other hand, the variation of NDVI levels is high among the different scales and devices used in our experiment. In the case of satellite images, NDVI values are in the range of 0.44 and 0.34 for Sentinel 2 and Landsat 8, respectively. For *in situ* spectral signatures, the NDVI range is close to 0.93, and with the GreenSeeker, it is 0.72. This variability is evident between different devices comparing these values with previous works. For example, [28] used an ADC Micro tetracam camera to calculate NDVI from images captured over avocado crops and obtained NDVI values around 0.95 for healthy trees and 0.90 for diseased trees. On the other hand, in [29], data from Sentinel 2 were used to calculate NDVI over an avocado production area in Kenya, obtaining average values of 0.38 for the dry season and 0.43 for the wet season.

4. CONCLUSIONS

This paper presents a characterization of the spectral response of avocado *(Persea Americana Mill cv. Hass)* from signatures captured in the visible to near-infrared range.60 young and 60 mature leaves were collected on four farms in Antioquia. A comparison between the spectral signatures collected directly over the leaves with data obtained from multispectral images captured by Sentinel 2 and Landsat 8, as well as an analysis of e the behavior of different VI.

The spectral signatures collected in close-range on avocado allowed us to determine a spectral difference between the young and old leaves. This difference is predominant in the range from 450 nm to 650 nm, and a shift of the red edge is evident. The range from 480 nm to 650 nm is also the most discriminant by an unsupervised band selection algorithm based on singular value decomposition.

On the other hand, spectral characterization using satellite data is more challenging. The signatures obtained using Sentinel 2 and Landsat 8 present several variations. These differences can result from the date of acquisition, the spatial resolution of the sensor, and the radiometric and atmospheric corrections of each system. In the case of Sentinel 2, an image with low cloud cover (less than 30%) was obtained on May 8, 2022. With the Landsat 8 system, the closest image to the date of capture of the leaf signatures and low cloud cover was obtained on January 8, 2022. In addition, the analysis is based on Sentinel 2 bands with a 10-meter spatial resolution, while the Landsat 8 bands correspond to a 30-meter spatial resolution. This implies that the pixels that obtain the characteristic spectral signatures present a mixture of materials. Although both images have radiometric and geometric corrections, the signatures vary significantly.

The studied VI, also evidences the differences between young and mature leaves in the spectral characterization using close-range spectrometry. Values close to 0.9 were obtained using the NDVI. However, more significant deviations are presented in younger leaves. Similar behaviors are obtained using MCARI and OSAVI indices. From satellite data, we only can compute two VI that uses the available spectral bands. In this case, the NDVI values are around 0.4 for Sentinel 2 and 0.3 for Landsat 8.

6. REFERENCES

Bibliographic references were omitted, but are in the original article. This is an internal disclosure.

Profesor
Andrés Felipe Vargas

Semillero chemtrónica del programa de Química Industrial

Chemtrónica fue el primer semillero del programa de Química Industrial, iniciando sus labores académicas y de investigación en el semestre 2016-2. En sus comienzos, nace con la idea de acercar a los estudiantes de química a la investigación aplicada, buscando que estos adquirieran destrezas en el manejo de los equipos de laboratorio y habilidades en las aplicaciones prácticas de la química.

Para el semestre 2017-1 se propone un cambio en el enfoque del semillero y se optó por orientar nuestras labores a la creación de hardware científico de bajo costo empleando plataformas de software y hardware abierto, esto con el fin de buscar la automatización de procesos químicos y la medición de variables fisicoquímicas. Para ello se seleccionó la plataforma abierta Arduino ®, tanto en hardware como en software, para la implementación y adecuación de equipo científico, con el fin de permitir a los estudiantes un acercamiento a la investigación, el pensamiento crítico y reflexivo, la programación, a los circuitos electrónicos y la solución de problemas.
En el semillero se han construido varios prototipos de equipos científicos de bajo costo, los cuales se describen a continuación.

Termómetro: para la elaboración y el desarrollo de este, se empleó un sensor de temperatura *Lm35* que por medio de Arduino realiza la lectura de temperatura a través de una conversión análoga-digital, y el valor de temperatura se muestra en el celular del usuario a usando conexión serial. La verificación de las temperaturas se realizó en el laboratorio empleando un baño de hielo a 0°C y el punto de ebullición del agua en Medellín 96 °C. *pHmetro:* en la fabricación de este instrumento, se empleó un sensor de pH de bajo costo y una pantalla de cristal líquido que usando los principios del anterior instrumento descrito, a través de conversión análoga-digital obtiene el valor del pH que posteriormente es mostrado en una pantalla. Para perfeccionarlo, se implementó la función de calibración empleando buffer de 4.01, 7.01 y 10.00 en el laboratorio de Química.

Bomba dosificadora: el control de velocidad de una bomba peristáltica a través de Arduino permite la dosificación de líquidos, lo que permite vigilar el flujo y la cantidad de líquido dosificado. Para la calibración de este instrumento se empleó una balanza analítica del laboratorio de Química.
Sensor de gases: en el desarrollo de este, se utilizó un sensor de gases de bajo costo, MQ135, con el objetivo de implementar un sistema de medición de gases, buscando este fin, se recurrió al Arduino utilizando un teclado y una pantalla LCD que permite elegir el gas a medir y mostrar la concentración del gas que se tiene. Adicionalmente se realizó una aplicación Android para recibir los datos de concentración del gas en tiempo real a través de WIFI.

Potenciostato: se construyó un potenciostato que permite seguir reacciones químicas de óxido-reducción a través de la medición de corriente y voltaje de estas, en el sistema se implementó un control y visualización a través de una pantalla con control táctil, que permite tanto la programación de los parámetros del experimento, como la visualización de los resultados en tiempo real.

Cabe resaltar esta valiosa labor académica de formación investigativa en los estudiantes, puesto que el semillero ha permitido la formación de varios alumnos que han realizado sus modalidades de grado en temas relacionados con las líneas investigativas del semillero. Esta primera aproximación ha permitido la participación de algunos de ellos como jóvenes investigadores en grupos de investigación de la institución y también la formación a nivel de posgrado después de culminar sus estudios de pregrado.

Esperamos haber llegado con este tercer boletín del año académico 2024, a la mayor cobertura del personal que hace parte del Departamento de Educación y Ciencias Básicas y de la Facultad de Ciencias Exactas y Aplicadas en general, con esta propuesta y esfuerzo que venimos desarrollando desde la actual dirección y coordinación del departamento.

NOTA *Si algún docente o estudiante desea aportar una información o nota para el próximo boletín, agradecemos se comunique al correo:*
Ramirohoyos@itm.edu.co
O al celular 315 410 62 62